Energy 254 (2022) 124308

Contents lists available at ScienceDirect

Energy

journal homepage: www.elsevier.com/locate/energy

Modelling and evaluation of a high-temperature heat pump two-stage cascade with refrigerant mixtures as a fossil fuel boiler alternative for industry decarbonization

Joaquín Navarro-Esbrí, Adrián Fernández-Moreno, Adrián Mota-Babiloni*

ISTENER Research Group, Department of Mechanical Engineering and Construction, Universitat Jaume I, Castelló de la Plana, 12071, Spain

ARTICLE INFO

Article history:
Received 29 December 2021
Received in revised form
10 May 2022
Accepted 15 May 2022
Available online 22 May 2022

Keywords:
High-temperature heat pumps (HTHP)
Low global warming potential (GWP)
Zeotropic mixtures
Semi-empirical model
Renewable energy
Greenhouse gas (GHG) emissions

ABSTRACT

High-Temperature Heat Pump (HTHP) is becoming a feasible technology for decarbonization, being proposed as an alternative to fossil fuel boilers in several industrial, commercial, and urban applications. This work presents a semi-empirical assessment of a two-stage cascade cycle for HTHP applications to produce hot water up to 150 °C from a water flow at 35 °C and 25 °C. This work uses experimental results of two single-stage heat pump prototypes (R-1234ze(E) and R-1336mzz(Z)) with different temperature lifts as baseline inputs. The energy performance of the proposed two stage cascade HTHP is evaluated through a semi-empirical model, including several novel mixtures for both stages. Up to 14% of COP increase was reached respect to the baseline when using R-152a/600 (0.08/0.92) and R-1233zd(E)/161 (0.88/0.12) for the low stage and high stage, respectively. The VHC increases 30% with the selected combinations, but the discharge temperature also rises. Direct CO_2e emissions were negligible by using low GWP refrigerants. The country proposed for the two-stage cascade HTHP greatly influences greenhouse gas indirect CO_2e emissions. It is estimated that in countries carbon emission factor lower than 0.35 $kgCO_2e\ kWh^{-1}$ the mixtures selected would reduce the emissions compared to fossil fuel boilers for the same heating capacity.

1. Introduction

High-temperature heat pumps (HTHPs) are suitable systems for waste heat recovery in various industrial processes. Still, the main market barriers are insufficient knowledge about the integration of HTHPs, the lack of available refrigerants in this temperature range with low global warming potential (GWP), and the high price ratio of electricity to fossil fuels [1]. According to Kosmadakis [2], the total potential of industrial heat pumps is 28.37 TWh per year in the EU. The necessary waste heat to be recovered by heat pumps is about 21 TWh per year, 7% of the total waste heat potential in EU industries. The most promising sectors are non-metallic minerals, food, paper, and non-ferrous metal. Heat pumps for producing heat up to 150 °C from a heat source below 100 °C have a specific equipment cost ranging from 150 to 300 € per kW, mainly depending on the cycle design and temperature. Moreover, the discounted payback period shows a large scatter and can be down to 3 years [3].

Several applications have already been studied. Urbanucci et al. [4] integrated an HTHP to recover heat from an absorption chiller and produce 90 °C hot water. This solution could save 10.3%, 10.6%, and 41.7% compared to traditional trigeneration, cogeneration, and separate production systems, respectively. Bargo-Burgos et al. [5] calculated an overall coefficient of performance (COP) between 3 and 4 for a commercial central heat pump and combined heat and power plant, and individual heat pumps located in a district heating and cooling network. Local heat pumps in 4th and 5th-generation district heating networks result in a 1.0 to 1.5 COP. Sharan et al. [6] proposed the integration of an HTHP to reduce the supercritical water desalination energy requirement. This combination was 20% more energy-efficient than the commercial systems for 25% feed concentration. In the UK food and drink industries, waste heat between 80 and 200 °C could save 164 $ktCO_2$ per year. Then, there is scope to save 2.6 $MtCO_2$ per year with projected 2030 grid electricity emissions factors [7]. Wu et al. [8] found the simultaneous maximization of HTHP heating capacity and annual net profits conflictive, so they proposed a decision-making method for the optimal result. At the optimal heat source inlet temperature of

* Corresponding author.
E-mail address: mota@uji.es (A. Mota-Babiloni).

https://doi.org/10.1016/j.energy.2022.124308

Nomenclature

Variables

COP	coefficient of performance (−)
k	heat capacity ratio (−)
$\dot{m}$	mass flow rate (kg s^{-1})
p	pressure (bar)
PR	pressure ratio (−)
$\dot{Q}$	heat transfer (kW)
h	specific enthalpy (kJ kg^{-1})
T	temperature (°C)
TEWI	total equivalent warming impact (tCO_2e)
VHC	volumetric heating capacity (kJ m^{-3})
$\dot{W}_c$	compressor's power consumption (W)
x_v	vapor quality (−)

Subscripts

k	condenser
cri	critical
o	evaporator
fg	heat of vaporization
in	inlet
i	intermediate
is	isentropic
out	outlet
suc	suction
vap	vaporization

Greek

η	efficiency (−)
ρ	density (kg m^{-1})
μ	viscosity (Pa s)

Abbreviatures

GWP	global warming potential
HTF	heat transfer fluid
HS	high temperature stage
HTHP	high-temperature heat pump
HFC	hydrofluorocarbon
IHX	internal heat exchanger
LS	low temperature stage
NBP	normal boiling point
ORC	organic Rankine cycle
SC	subcooling
SH	superheating

71 °C and condensing temperature of 145 °C, the system's heating capacity was 499 kW, and the payback period was 3.9 years.

Single-stage cycles with an internal heat exchanger (IHX) are economically favored at temperature lifts up to 50 K, whereas above this value, two-stage cycles show superior cost-effectiveness [3]. Jung et al. [9] experimentally investigated an R-410A/R-134a cascade for air heating with a hot water supply. This system showed more stable air and water heating operations and higher water outlet temperatures than a single-stage R-410A heat pump. Zou et al. [10] focused on temperature stage matching of a cascade air source heat pump with vapor injection. A prototype using R-245fa and R-410A produced heat at 140 °C, and the COP varied from 1.2 to 1.6 at ambient temperatures from −10 to 20 °C. Xu et al. [11] developed a similar system in residential and industrial hot water (55–75 °C) at low ambient temperatures (−20 °C) [11]. The results reveal adequate energy, economic, and environmental performance compared to other technologies.

Bergamini et al. [12] showed that HTHPs are promising substitutes for gas boilers for heat production up to 180 °C, but the working fluid is vital. R-717 was preferable for heat source and sink temperatures lower than 60 and 110 °C, respectively, while R-718 at higher values. According to Wu et al. [13], R-718 has better performance than R-1336mzz(Z) at higher condensation temperatures, more safety than R-600, and higher output temperature with lower GWP than R-245fa. However, it still requires suitable technology for compressors and reducing discharge temperatures.

Mikielewicz and Wajs [14] assumed a heat source temperature of 50 °C and a condensation temperature is 130 °C and concluded that ethanol proved to be the best fluid in a single-stage configuration. R-601 and R-365mfc have limited application because of higher flammability and price. Frate et al. [15] recommended acetone, benzene, dichloroethane, and cyclopentane for different heat source and heat sink temperatures. If lack of toxicity or flammability is imposed to deploy HTHPs, synthetic refrigerants R-1336mzz(Z), R-1234ze(Z), R-1233zd(E), and R-1224yd(Z) are also attractive, but with a 20% energy performance decrease.

Focusing on pure organic refrigerants, Yan et al. [16] developed a simple model for single stage HTHPs involving newer working fluids such as R-1336mzz(Z) and R-1224yd(Z). The inputs were critical temperature and pressure; the outputs, specific volumetric heating capacity (VHC), and COP. Zhang and Xu [17] carried out experimental tests with R-134a, R-227ea, R-236fa, R-245fa and R-1234ze(Z) in the condensation temperature range of 70–85 °C. The COP of R-1234ze(Z) was 3.55 at the highest condensation temperature, and the temperature lift of 45 K. Luo and Zou [18] simulated several cycles and refrigerants. The most efficient configurations were the expander cycle and IHX cycle regarding COP and volumetric heating capacity. R-245fa, R-600 and R-1234ze(Z) presented comparable COP, but a notable VHC increase employing R-600, R-600a and R-1234ze(Z) instead of R-245fa was highlighted. Malavika et al. [19] recommended an HTHP with R-1233zd(E) for an industry with both process heating and cooling demands. The cost, as well as the overall energy consumption, can be decreased. Mateu-Royo et al. [20] fixed the heat source temperature at 80 °C, whereas the heat sink temperature varied from 110 to 140 °C to assess the R-1224yd(Z) theoretical and semi-empirical adaptation. Its heating capacity was 9% lower than R-245fa, but the COP increased up to 4.5%, reducing 90% the CO_2e emissions.

A few papers can be found regarding studies with the combined effect of advanced configurations and organic refrigerants. All of them confirmed benefits in energy performance at high HTHP temperature lifts. Jiang et al. [21] theoretically obtained that when recovering 50 °C waste heat and supplying 60–130 °C hot water, R-1233zd(E) increases heating capacity from 2.1 to 2.2 MW and decreases COP from 23.0 to 2.9. Besides, at 80 °C waste heat and 90–160 °C hot water, the heating capacity increases from 4.1 to 4.2 MW, and the COP decreases from 24.4 to 4.6. These simulations confirmed the energy performance degradation with a single cycle at higher production temperatures. Dai et al. [22] compared five dual-pressure condensation HTHP configurations with traditional single-stage, two-stage, and cascade HTHP systems to improve thermal matching in the heat sink. The COP of the dual-pressure condensation water-cooled saturated system is the highest (4.2), 3%–9% higher than traditional HTHPs. R-1234ze(Z) showed higher

energy performance than the rest. Mateu-Royo et al. [23] compared different advanced configurations, being the two-stage cascade the most suitable for higher temperature lifts. Mateu-Royo et al. [24] proposed a reversible HTHP and Organic Rankine Cycle (ORC) that achieves a COP of 2.44 for condensing temperature of 140 °C, operating in HTHP mode. In contrast, the ORC mode provides a net electrical efficiency of 8.7% at condensing temperature of 40 °C. Besides, R-1233zd(E) and R-1224yd(Z) provide COP and electrical net efficiency improvements, higher in the first case.

Then, a few mixtures for HTHPs have also been proposed in single-stage HTHPs. Xu et al. compared R-245fa binary mixtures at different HTHP conditions. At a heat sink temperature of 100 °C, the COP of a prototype mixture was approximately 4.9, higher than that of R-245fa. This mixture also presented the lowest overall system exergy destruction and extra cost rate [25]. Ma et al. [26] proposed a near-zeotropic mixture with unknown composition, BY-3, for the low-temperature stage of a two-stage cascade using R-245fa in the high-temperature stage. Numerical models and experiments proved that this refrigerant pair could produce hot water at 142 °C, and the temperature lift could be 100 °C. Zühlsdorf et al. [27] optimized a heat pump for a large temperature glide on the heat sink and a smaller temperature glide on the heat source. They considered a numerical simulation of binary mixtures based on a list of 14 natural refrigerants and determined an increase in performance up to 20% for a single stage cycle and up to 27% if the superheating can be avoided. Mateu-Royo et al. [28] considered R-1234ze(E) and R−515B as low GWP alternatives to R-134a for reaching condensation temperatures of 85 °C at comparable COP.

There is a recent interest in heat pumps to be powered by renewable energy; however, the technology is not still ready to enter definitively into the market. Research about heat pump technology, configurations and refrigerants is required. Two-stage cascades allow covering high-temperature lifts without needing a higher temperature heat source. Moreover, the energy performance can be improved by using novel mixtures in both stages.

This work focuses on the HTHP technology as a viable alternative to fossil fuel boilers. Experimental results of single-stage heat pumps operating at different temperature levels are integrated and combined to simulate a two-stage cascade HTHP. Therefore, a semi-empirical model is developed using R-1234ze(E) and R-1336mzz(Z) measurements. This model is validated, and then it is used to simulate the operation of prototype mixtures optimized in previous studies in both temperature levels. Semi-empirical results with mixtures are compared regarding COP and distinguishing GWP and flammability levels. Finally, the refrigerant pair with the highest energy performance is selected. The carbon footprint is calculated using the total equivalent warming impact (TEWI) metric and compared with a fossil fuel boiler. The following section presents the configurations and refrigerants studied. Then, the experimental setups are briefly exposed. In the following, the methodology description includes an experimental campaign and semi-empirical modelling. The results corresponding to performance and environmental analysis are shown in the fifth section. Finally, the conclusions summarize the main results obtained.

2. Configuration and refrigerants

2.1. Two-stage cascade with internal heat exchangers

In this section, the configuration and refrigerants are presented. The scheme and pressure-enthalpy (P-h) diagram of the cascade HTHP is shown in Fig. 1. Two basic cycles with an IHX are connected by a cascade heat exchanger, operating as the evaporator for the high-temperature stage (HS) and condenser in the low-temperature stage (LS). Cascade configurations allow increasing the temperature lift typically covered by vapor compression systems with an acceptable pressure ratio by splitting it into two compressors. Moreover, other parameters such as discharge temperatures, operating pressures, and compressor efficiencies are improved by this construction.

2.2. Baseline refrigerants

The refrigerants selected in this work are R-1234ze(E) for the LS and R-1336mzz(Z) for the HS. The main properties of both refrigerants are shown in Table 1.

Both refrigerants have a low global warming potential and zero ozone depletion potential, as required to future-proof substances.

Table 1
Main properties of the refrigerants used as a reference.

Refrigerant	R-1234ze(E)	R-1336mzz(Z)
Cascade stage	LS	HS
ASHRAE safety class	A2L	A1
Molar mass [g·mol^{-1}]	114.0	164.1
P_{crit} [MPa]	3.63	2.90
T_{crit} [°C]	109.4	171.3
$GWP_{100\text{-}yr}$	<1	2
Δh_{vap} [kJ·kg^{-1}]	163.1	136.3
Δh_k [kJ·kg^{-1}]	93.4	78.2

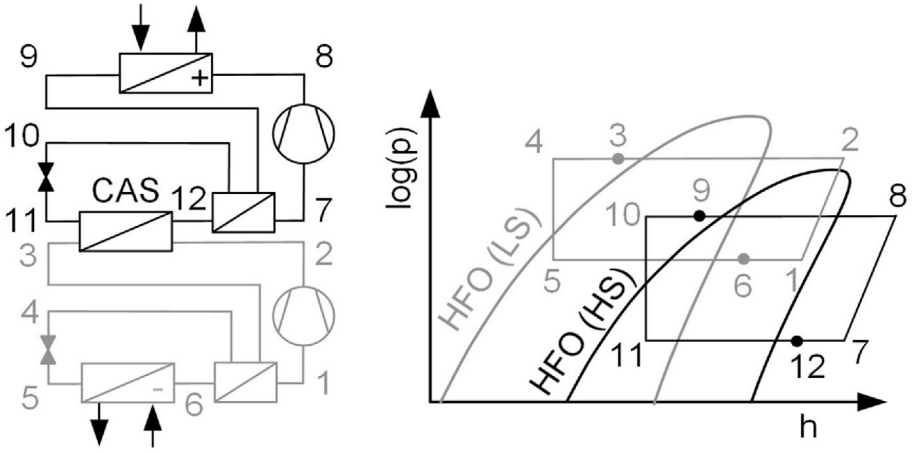

Fig. 1. Schematic representation and P-h diagram of the two-stage cascade HTHP.

The refrigerant used in the HS presents no flame propagation (A1), while the LS is mildly flammable (A2L). A cascade would reduce the risk of using an A2L refrigerant, restricting the flammable refrigerant to the LS. Moreover, R-1336mzz(Z) is only a lower toxicity refrigerant, in contrast with R-245fa, typically proposed in commercial HTHPs and a higher toxicity fluid. There is a significant difference in the temperature and critical pressure between both fluids, making them suitable for the proposed stages and operating conditions. R-1234ze(E) is one of the R-134a alternatives with the highest critical temperature, allowing a high energy performance even at high condensation temperatures. The same happens for R-1336mzz(Z), which can be used for HTHPs without operating at transcritical conditions. The latent heat of vaporization and condensation of R-1336mzz(Z) and R1234ze(E) indicate that both could require a similar mass flow rate.

2.3. Potential mixture refrigerants

The literature was investigated to select potential refrigerant combinations for a HTHP cascade. For the LS, the main criterion was that the authors proposed those mixtures as potential candidates for future medium-scale applications (potential alternatives to R-134a). The works of Thu et al. [29], Wang et al. [30], Li et al. [31] and Calleja-Anta et al. [32] fitted better this criterion (numbered following the prefix LS). For the HS, the selected fluids were taken from a previous study that investigated mixtures for HTHPs [33].

All relevant properties, including the estimated flammability class based on the method proposed by McLinden et al. [34], are shown in Table 2. Thermodynamic properties of refrigerants are retrieved from REFPROP v10.0 [35]. All the LS mixtures have their NBP below ambient temperature. LS4 and LS5 have lower critical temperatures, restricting their operable condensing temperatures to 70 °C. LS8, LS9 and LS10 have significantly higher critical temperatures than the same stage because their main component is R-600. Most of them are ultralow GWP, except LS2, LS3 and LS6, which have GWPs of around 150.

On the other hand, for the HS, all the mixtures have a critical temperature above 160 °C. This feature makes these mixtures appropriate for working at high temperatures such as 150 °C in the condenser. Most of them have their NBP between 0 and 40 °C, so their pressure on the vessels would be less than 1 atm. All the mixtures in the HS have GWPs under 25.

Fig. 2 shows the p-h and T-s diagrams for the LS and HS. As seen in Fig. 2 (a) and (b), most of them have similar behavior, except LS8, LS9 and LS10, which are significantly different as they are mixtures based on R-600, with a higher latent heat of vaporization/condensation. This could imply higher energy performance of the alternative refrigerants, but the flammability is still a concern. Additionally, in Fig. 2 (c) and (d), the behavior in the diagrams is even closer. The baseline R-1336mzz(Z) has one of the lowest latent heat of vaporization/condensation.

3. Experimental setup

This section shows the test benches used from which the experimental results were retrieved and later used to simulate the cascade performance. These facilities consist of two basic cycles with IHX designed to operate at moderate and high temperatures. The description of the main components of each test bench is shown in Table 3.

The experimental setup aimed to simulate the LS is a fully monitored vapor compression system with an IHX and two secondary closed-loop circuits that provide the thermal load (evaporator) and heat dissipation (condenser). When the targeted steady-state point is reached, the test is recorded for 10 min with a sample period of 5 s. The scheme and picture are shown in Fig. 3.

For the secondary circuits, a closed-loop propylene glycol-based circuit (heat load) is composed of a variable speed pump, a 100 L storage buffer tank, and three 5.6 kW resistances which actuation is controlled to set the evaporating temperature with a PID. Additionally, the other closed-loop water-based circuit (heat removal) has a variable speed pump and a frequency-controlled fan coil that allows setting the condensing temperature.

The HS is simulated by means of a fully monitored single-stage HTHP with IHX. The targeted steady-state points are recorded when heat sink and source temperatures stabilize for 5 min, with a sampling period of 1 s. The maximum deviation for the sink and source temperatures was 0.3 °C and 0.15 °C, respectively. Two secondary circuits are used to set the targeted evaporation and condensation temperatures based on thermal oil as heat transfer fluid. The heat sink's secondary fluid is thermal oil, which is cooled in a water-cooling circuit controlled by a PID that assures the heat sink's thermal stability with a dry cooler. Heat source resistances employed to simulate waste heat source are controlled by a PID in an electric boiler.

Table 2
Mixtures studied as refrigerants for a HTHP cascade.

Designation	Composition	GWP[a]	T_{cri} (°C)	p_{cri} (bar)	NBP (°C)	Safety class[c]	Reference
LS1	R-1234ze(E) pure	1.00	109.36	36.35	−18.97	A2L	Baseline
LS2	R-1234yf/32/744 (0.72/0.22/0.06)	155.66	89.98	43.75	−49.89	A2L	Thu et al. [29]
LS3	R-32/1234ze(E) (0.3/0.7)	211.9	105.32	46.83	−39.00	A2L	Wang et al. [30]
LS4	R-32/1123/13I1 (0.2/0.5/0.3)	141.42	71.23	48.76	−58.52	A2L	Yu et al. [30]
LS5	R-1123/161/13I1 (0.65/0.05/0.3)	1.26	72.94	45.50	−56.15	A2L	Yu et al. [30]
LS6	R-134a/1234ze(E) (0.11/0.89)	150.49	108.07	36.87	−20.34	A2L	Li et al. [31]
LS7	R-152a/1234ze(E) (0.5/0.5)	74.5	107.78	40.00	−23.70	A2L	Li et al. [31]
LS8	R-152a/600 (0.08/0.92)	15.52	146.97	40.19	−14.64	A3	Calleja-Anta et al. [32]
LS9	R-1234yf/600 (0.1/0.9)	3.7	144.56	39.34	−15.05	A3	Calleja-Anta et al. [32]
LS10	R-1234ze(E)/600 (0.09/0.91)	3.73	145.97	39.04	−9.56	A3	Calleja-Anta et al. [32]
HS1	R-1336mzz(Z)	2	171.35	29.03	33.45	A1	Baseline
HS2	R-1336mzz(Z)/152a/601 (0.8/0.16/0.04)	25.52	165.62	33.77	6.25	A1	Fernández-Moreno et al. [36]
HS3	R-1233zd(E) pure	1	166.45	36.24	18.26	A1	Fernández-Moreno et al. [36]
HS4	R-1233zd(E)/601/152a (0.65/0.25/0.1)	16.95	165.75	37.41	7.13	A2L	Fernández-Moreno et al. [36]
HS5	R-601/1234ze(Z) (0.74/0.26)	4.7	178.77	35.97	15.31	A3	Fernández-Moreno et al. [36]
HS6	R-1233zd(E)/152a (0.86/0.14)	21.58	160.04	38.85	2.94	A1	Fernández-Moreno et al. [36]
HS7	R-1233zd(E)/161 (0.88/0.12)	2.32	161.10	39.55	−2.26	A1	Fernández-Moreno et al. [36]
HS8	R-601 pure	6	196.55	33.68	36.06	A3	–

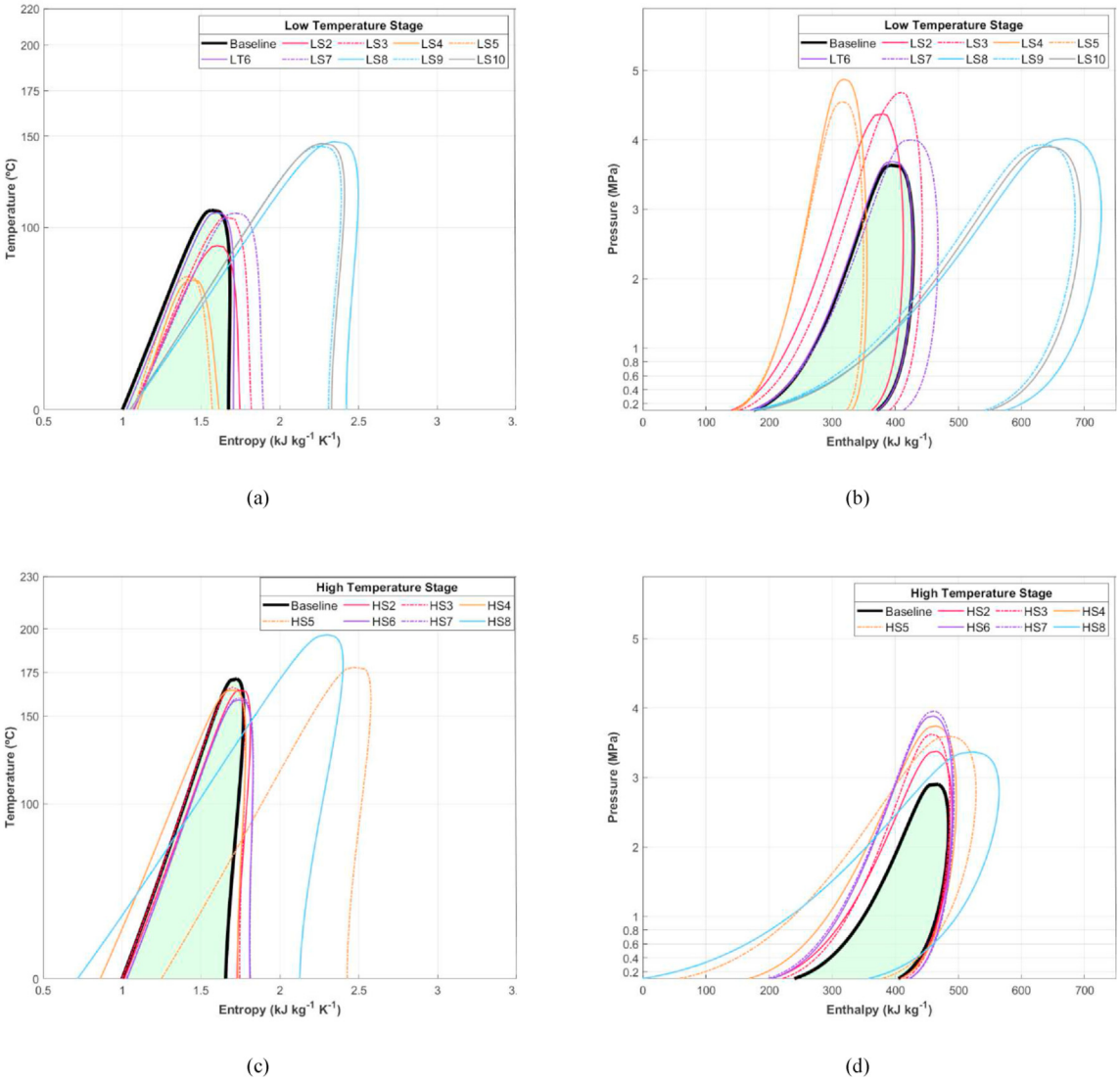

Fig. 2. Pressure-enthalpy and temperature-entropy diagrams for the LT (a,b) and HT (c,d) candidates.

Table 3
Main component description for the low stage and high stage cycle.

Component	Description for low stage	Description for high stage
Compressor	Danfoss scroll compressor, 17.3 kW at 50 Hz, swept volume of 114.5 cm^3, operational temperatures between 50 and 155 °C.	Magnetically coupled compressor, 7.5 kW at 50Hz, swept volume of 121.1 cm^3. Modified for high temperatures.
Condenser	Brazed plate type, 40 plates, heat exchange area of 2.39 m^2	Brazed plate type, 86 plates, heat exchange area of 5.29 m^2
Evaporator	Brazed plate type, 24 plates, heat exchange area of 1.39 m^2	Brazed plate type, 48 plates, heat exchange area of 6.07 m^2
Internal heat exchanger	Brazed plate type, 30 plates, heat exchange area of 0.336 m^2	Brazed plate type, 50 plates, heat exchange area of 3.02 m^2
Expansion valve	Electronic expansion valve	Electronic expansion valve

A picture of the system and a scheme are shown in Fig. 4. The details about the sensors and uncertainties are shown in Table 4, and the error propagation analysis has been carried out with the software Engineering Equation Solver [37].

Temperatures, pressures, flow rates and power consumptions are measured in the main and secondary circuits. The thermodynamic states of the refrigerants are determined using REFPROP v10.0 [31].

4. Methodology

4.1. Experimental measurements

The test campaign covered a wide range of temperatures, as shown in Table 5. The aim is to provide a wide range of points for calculating the experimental COP and developing the semi-empirical model. The highest outlet sink temperature (heat sink outlet) in the HS was 160 °C. The heat source temperature in the LS

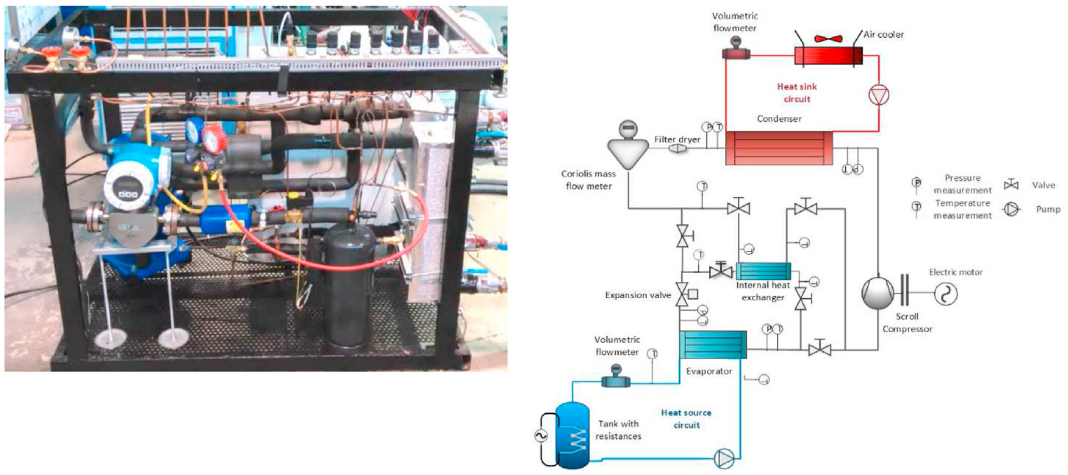

Fig. 3. Experimental setup for the simulation of the low-temperature stage.

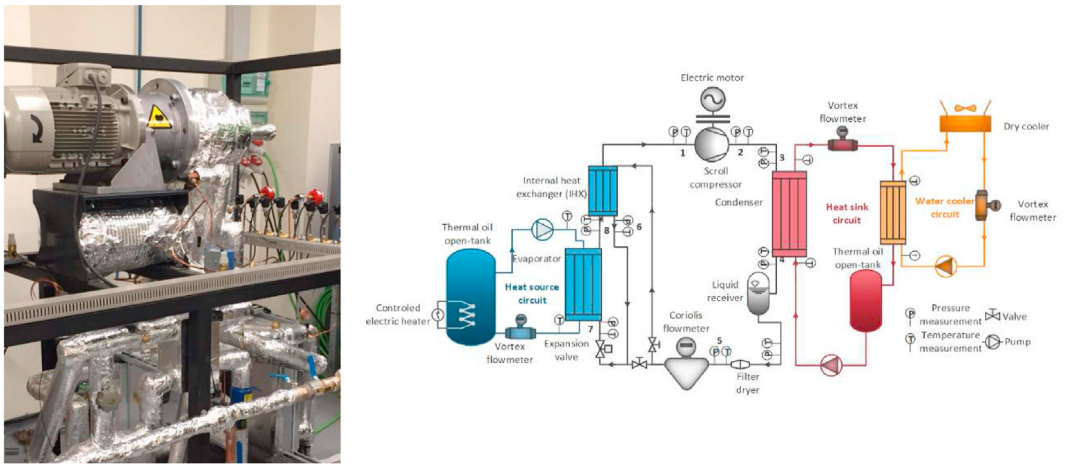

Fig. 4. Experimental setup for the simulation of the HS cycle.

Table 4
Overview of sensors uncertainties (relative uncerainty refers to reading).

Measured parameters	Sensor	Uncertainty
Low Stage		
Temperatures	K-type thermocouples	±0.3 K
Pressures	Piezoelectric pressure transducers	±0.15%
Refrigerant mass flow rate	Coriolis mass flowmeter	±0.1%
Heat source volumetric flow rate	Electromagnetic flowmeter	±0.33%
Water cooler volumetric flow rate	Electromagnetic flowmeter	±0.114 $m^3\ h^{-1}$
Compressor power consumption	Digital wattmeter	±1.55%
High Stage		
Temperatures	J-type thermocouples	±0.3 K
Pressures	Piezoelectric pressure transducers	±0.04%
Refrigerant mass flow rate	Coriolis mass flow meter	±0.17%
Heat source volumetric flow rate	Vortex flowmeter	±0.5%
Heat sink volumetric flow rate	Vortex flowmeter	±0.028 $m^3\ h^{-1}$
Compressor power consumption	Digital wattmeter	±1.55%

Table 5
Experimental temperature ranges for LS and HS cycles.

Temperature	Low-temperature stage	High-temperature stage
Inlet heat source (°C)	25–40	80–118
Outlet heat source (°C)	15–30	70–90
Outlet sink temperature (°C)	55–90	100–160

varied from 25 to 40 °C in the inlet and from 15 to 30 °C in the outlet of the evaporator to simulate the different ambient conditions.

Fig. 5 shows the experimental COP achieved for the different outlet sink temperatures. It is seen that the higher the outlet sink temperature, the lower the COP (higher pressure ratio). Three heat source temperatures were tested for the LS cycle, Fig. 5 (a). On the other hand, the temperature lift was constant for the HS cycle, Fig. 5 (b), so only one curve was given.

4.2. Semi-empirical model

When developing the semi-empirical model, its range of validity must be defined. This range is defined by the maximum, minimum

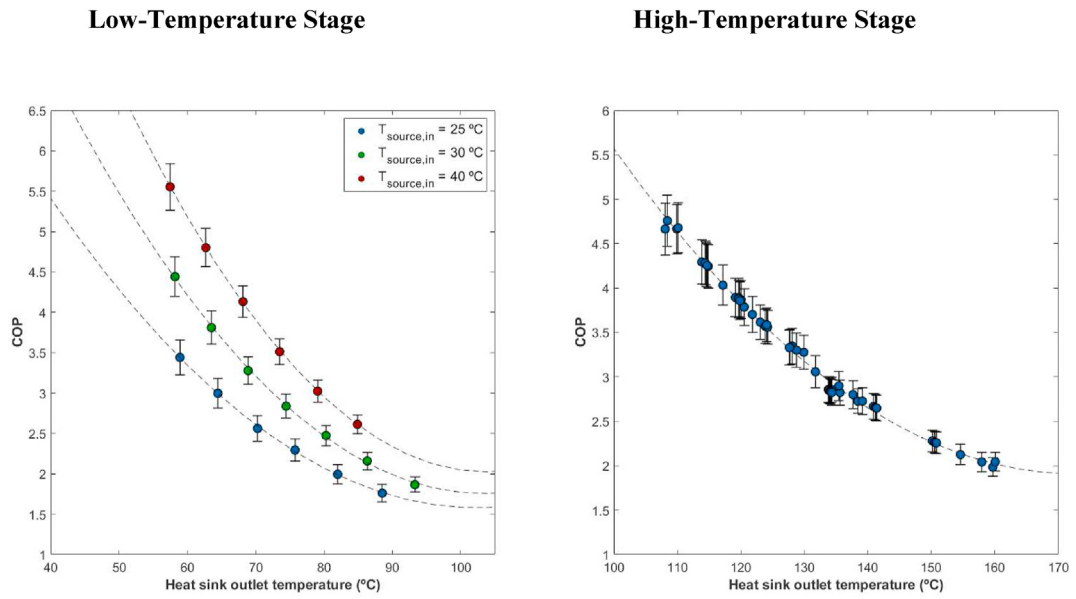

Fig. 5. Experimental implication between outlet sink temperature and COP for the low-temperature stage (a) and the high-temperature stage (b).

and intermediate temperatures. The maximum temperature is the highest temperature reached at the outlet sink temperature, and the minimum temperature is the lowest temperature reached at the inlet of the heat source circuit. On the other hand, the intermediate temperature is defined using Eq. (1) and considering a 2.5 K difference between the LS condenser and the HS evaporator. From the temperature ranges shown in Table 3, the operating range for the intermediate temperature is [78.5, 88.5] °C.

$$T_i = \frac{T_{out,o,HS+} T_{in,k,LS}}{2} \tag{1}$$

The same method for developing the semi-empirical model has been followed for both stages. Pressure drops are calculated with Eq. (2) as a function of the mass flow rate. Then, the temperature difference between heat transfer fluid and refrigerant is established at 3 K.

$$\Delta p = f(\dot{m}_r) \tag{2}$$

The compressor discharge temperature is obtained as a function, based on experimental data [38,39], of the suction conditions and the discharge pressure, as shown in Eq. (3).

$$T_{disch} = f(T_{suc},\ P_{suc},\ P_{dis}) \tag{3}$$

This method is employed for the baseline conditions. For the comparison between refrigerants, additional calculations consider refrigerant thermodynamic and transport properties. A figure of merit (FOM) is used for the pressure drop, as shown in Eq. (4), which considers viscosity and latent heat of vaporization. This FOM is applied to the baseline and the other refrigerants to modify the pressure drop correlation previously developed.

$$FOM_{\Delta p} = \frac{\mu^{1/4}}{\rho h_{fg}^{7/4}} \tag{4}$$

Finally, the energy performance parameters are determined. The heating capacity is fixed at 10 kW for the subsequent comparison with a boiler. Eq. (5) computes the electricity absorbed by the compressor as the isentropic enthalpy difference divided by the global efficiency. The COP is calculated using the heating capacity and the compressor power consumption as in Eq. (6). Following the results provided by Shungarov et al. [40], which tested the efficiencies of several scroll compressors, the global efficiency is taken as a constant for a pressure ratio between 3 and 5.5. This is confirmed by the experimental results and the validated model.

$$\dot{W}_c = \frac{(h_{is} - h_{suc})}{\eta_{glob}} \dot{m}_r \tag{5}$$

$$COP = \frac{\dot{Q}_k}{\dot{W}_{c,LS} + \dot{W}_{c,HS}} \tag{6}$$

The energy performance of the double-stage cascade HTHP is obtained from two points of view: experimental (for pure refrigerants used as a baseline) and semi-empirical (for the proposed mixtures and based on the experimental measurements). The expansion valve process is considered as isenthalpic, and other pressure drops and heat losses to the ambient are neglected.

4.3. Operating conditions

The cascade heat exchanger assumes a temperature lift of 2.5 K between condensing and evaporating temperatures. The inlet and outlet temperature at the condenser of the secondary fluid (thermal oil) varies from 100 to 140 °C and from 110 to 150 °C, respectively. Then, for the evaporator, the inlet and outlet temperatures of the secondary fluid (water) vary from 25 to 35 °C and from 15 °C to 25 °C, respectively. All details of the simulation are given in Table 6.

Table 6
Assumptions and boundary conditions used in modelling simulation.

Parameter	Assumed value
Heat sink outlet temperature ($T_{sink,out}$)	110, 130, 150 °C
Heat source inlet temperature ($T_{source,in}$)	25, 35 °C
Superheating degree (ΔT_{SH})	5 K
Subcooling degree (ΔT_{SC})	2 K
Condenser approach temperature ($\Delta T_{pp,sink}$)	2.5 K
Evaporator approach temperature ($\Delta T_{pp,source}$)	2.5 K
Heat sink temperature glide (ΔT_{sink})	10 K
Heat source temperature glide (ΔT_{source})	10 K

5. Results and discussion

5.1. Model validation

For the validation of the model, the same stationary points recorded experimentally were used as input parameters of the model. An acceptable model should have ±10% of deviation from the experimental points. This can be seen in Fig. 6, where the parameters that determine the energy performance, heating production and power consumption are within this limit.

Then, simulated results for temperatures between the lowest and the highest experimental conditions present a ±10% maximum deviation.

5.2. Performance analysis

All the refrigerants employed were combined in the different boundary conditions to conclude the best pair in the different ranges. Additionally, the intermediate temperature is optimized from 77.5 to 87.5 °C to provide the highest COP. Fig. 7 shows the different semi-empirical COP and pressure ratio (PR) values for an outlet sink temperature of 130 °C and outlet heat source temperature of 25 °C. Most of the combinations overperform the baseline, but not significantly. The baseline results show that 130 °C heating can be produced with a COP of 1.79, representing a 79% increase over electrical boilers. Regarding refrigerant mixtures, an 8% higher

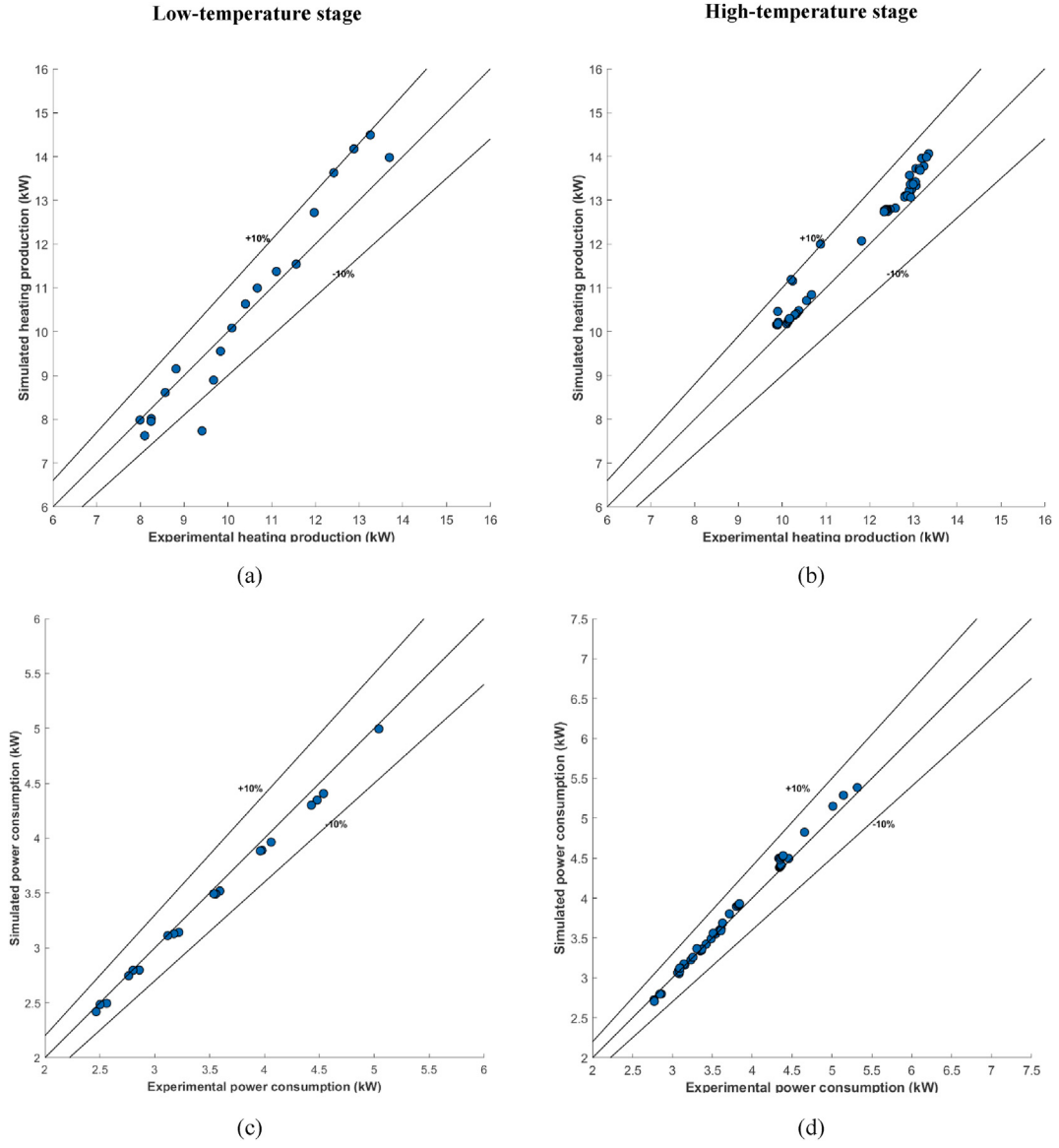

Fig. 6. Validation of heating production and compressor power consumption for the (a,b) LS and (c,d) HS.

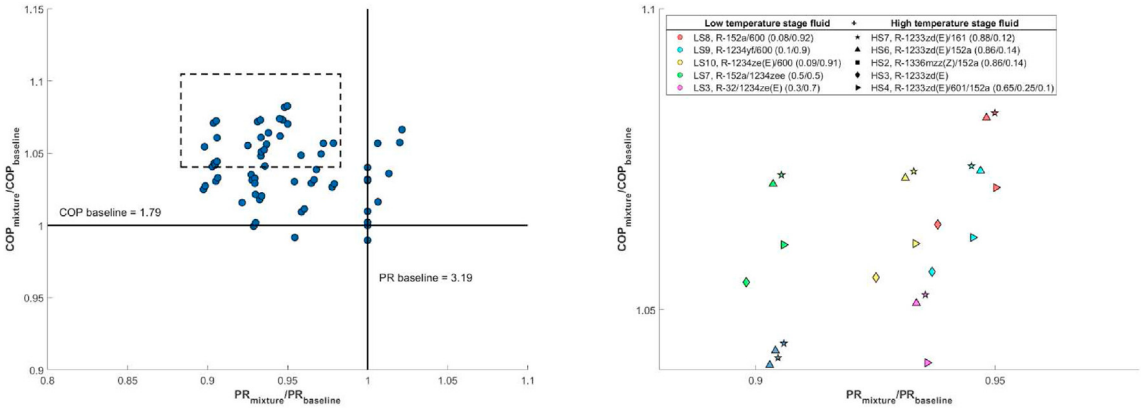

Fig. 7. COP as a function of the pressure ratio for all the combinations of mixtures in (a) HS and (b) LS.

COP than the baseline is expected for the combination of R-600/R-152a + R-1233zd(E)/R-161 (LS8+HS7). Then, other combinations showing remarkable increase are R-600/R-152a + R-1233zd(E)/R-161 (LS8+HS6). Their higher critical temperature respect to the baseline is traduced on a higher heat of vaporization and a decrease in the PR, reducing the irreversibilities of the compression process and then increasing the COP.

Thus, Fig. 8 shows the dominance of refrigerants in the LS (a,b) and HS (c,d). A higher radial value means that a component provides a higher COP value in combination with refrigerants of the

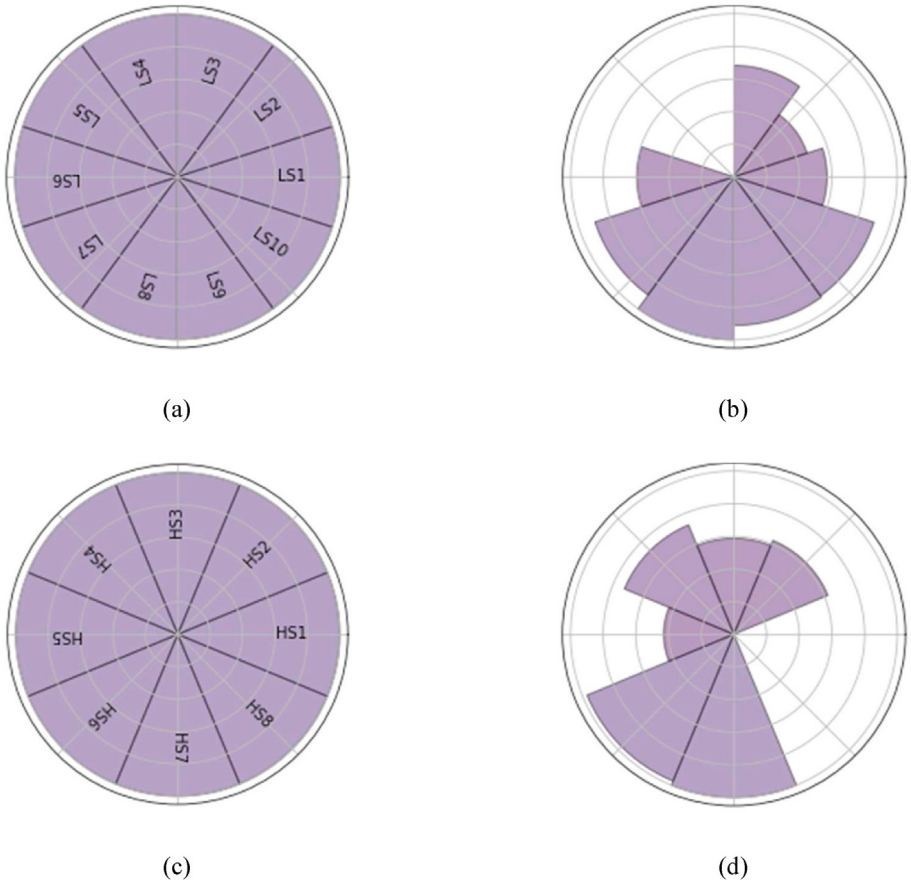

Fig. 8. Polar histogram of COP values for the different combinations of refrigerants in the LS (a,b). Higher values on the radial axis mean that all combinations with different refrigerants of the other stage have higher COP.

Table 7
Main parameters of the baseline cascade.

	Boundary condition	*COP*	*VHC* (kJ m^{-3})	*PR*	$\dot{m}_r$ (kg s^{-1})	T_{disch}
B1	T_{prod} = 110 °C $T_{source,\ in}$ = 35 °C	2.10	3248	2.08	0.071	115.1
B2	T_{prod} = 130 °C $T_{source,\ in}$ = 35 °C	1.79	2841	3.79	0.079	136.0
B3	T_{prod} = 150 °C $T_{source,\ in}$ = 35 °C	1.50	2624	4.69	0.084	162.0
B4	T_{prod} = 110 °C $T_{source,\ in}$ = 25 °C	1.80	3250	2.08	0.071	115.1
B5	T_{prod} = 130 °C $T_{source,\ in}$ = 25 °C	1.58	2842	3.18	0.080	136.1
B6	T_{prod} = 150 °C $T_{source,\ in}$ = 25 °C	1.35	2623	4.34	0.085	162.5

other stage. The most dominant mixture (usually resulting in high COP) for the LS is LS8, followed by LS9 and LS10, highly flammable refrigerants. If flammability is a concern, the mixture R-32/1234ze(E) (LS3) is the most convenient for the A2L flammability class. The other A2L mixtures with high COP are R-1234ze(Z) (baseline) and LS3. It is also seen that LS4 and LS5 are the ones with the lowest COP for this application, as their low critical temperature implies low COP and supercritical operational mode, which could not be estimated.

For the HS, two mixtures have higher COP than the rest. HS7 and HS6, both mixtures with low GWP and estimated flammability class A1, show higher COP. These two mixtures based on R-1233zd(E) have lower PRs and consequently a lower specific compressor work. Moreover, their latent heat of vaporization is higher than the baseline, leading to a COP increase. Then, HS4, an R-1233zd(E) based mixture, is the next in terms of COP. It is highlighted that the baseline, R-1336mzz(Z), presents the lowest COP. This is coherent with the results presented by Fernández-Moreno et al. [33]. Regarding this theoretical approach, all mixtures presented higher COP than R-1336mzz(Z).

The baseline results for the boundary conditions presented in Table 5 can be consulted in Table 7. A 2.10 COP is achieved for B1, which is the lowest temperature lift. Comparable COPs are obtained for B2 and B4. This means that a lower inlet temperature affects more the COP than a higher outlet sink temperature. This system could perform much better in warmer climates than in cooler. It is also important to consider the discharge temperature, as it should not be higher than 175 °C to maintain the working fluid chemical stability.

Eight combinations of mixtures for the LS and HS were taken as the most promising for future applications. Four with no flammability restrictions and four with estimated flammability class A2L or A1. Their main energy and operational parameters compared to the baseline can be observed in Fig. 9. This combination of mixtures shows a higher COP in all conditions. Additionally, the required mass flow rate would be lower, which would result in lower pressure drops, and the PR would be lower too. It is highlighted that the higher the temperature lift is, the higher the increase in COP would be.

On the other hand, boundary conditions B3 and B6 present a particular issue. As commented before, discharge temperature should not exceed 175 °C, and seven of the eight combinations selected do not fulfil this criterion. Through this, only the combination LS3+HS3 would be suitable for outlet sink temperatures of 150 °C, but the performance would be lower. This would be solved if the total superheat is reduced by limiting the total superheating degree or the IHX efficiency in future experimental works.

Through this, it can be seen that even if R-1234ze(E) and R-1336mzz(Z) are suitable low-GWP alternatives, potential mixtures have a higher potential regarding their thermophysical properties. The increase in performance is not exceptional, but it is considered sufficient for future HTHP proposals.

5.3. Environmental analysis

The environmental analysis of vapor compression systems usually comprises the carbon footprint caused by the installation during the normal operation and the refrigerant recovery losses. This two-stage cascade configuration has been based on ultra-low GWP refrigerants, and therefore, the direct emissions (caused by refrigerant leakages) are almost negligible. All the combinations proposed to improve the cascade also have low GWP. Therefore, the yearly carbon footprint of the installation considers the indirect emissions caused by the carbon emission factor of the electricity mix and the direct emission through leakages.

Five combinations of refrigerants are included in the environmental analysis: the baseline, two with at least one fluid of the cascade with a higher flammability class than the baseline, and two with the same flammability class as the baseline (A1 in HS and A2L in LS).

Table 8 shows the energy performance results required for obtaining the operational carbon footprint of the HTHP cascades to cover a 10 kW heating capacity.

Table 9 shows the carbon emission factor per country. Representative scenarios with different values of European countries carbon emission factor have been considered to obtain the condition in which the cascade HTHP would be more interesting.

Then, Table 10 includes the values required to obtain a natural gas boiler carbon footprint for the same thermal requirement.

Fig. 10 shows the cascade carbon footprint results using five combinations of refrigerants. For the baseline, countries with a carbon emission factor lower than 0.35 kgCO_2e kWh^{-1} reduce carbon emissions compared to the natural gas boiler. This system would still not be competitive in countries like Netherlands and Poland, which have higher emission factors. For countries with a low carbon emission factor, such as Sweden, the difference in carbon footprint is also negligible between the low GWP options, and the most convenient refrigerant combination should follow other considerations not limited to parameters derived from the thermodynamic operation, such as low cost and size of the installation, or global safety, among others.

On the other hand, the TEWI is estimated in the same conditions for an R-134a + R-245fa cascade. The aim is to study the effect on TEWI of using low GWP refrigerants against high GWP ones. The results presented in Table 11 show that the reduction in carbon emissions in countries with higher carbon emission factors is slight. That is to say, direct emissions are negligible in comparison. However, in countries like Spain, the reduction in carbon emissions

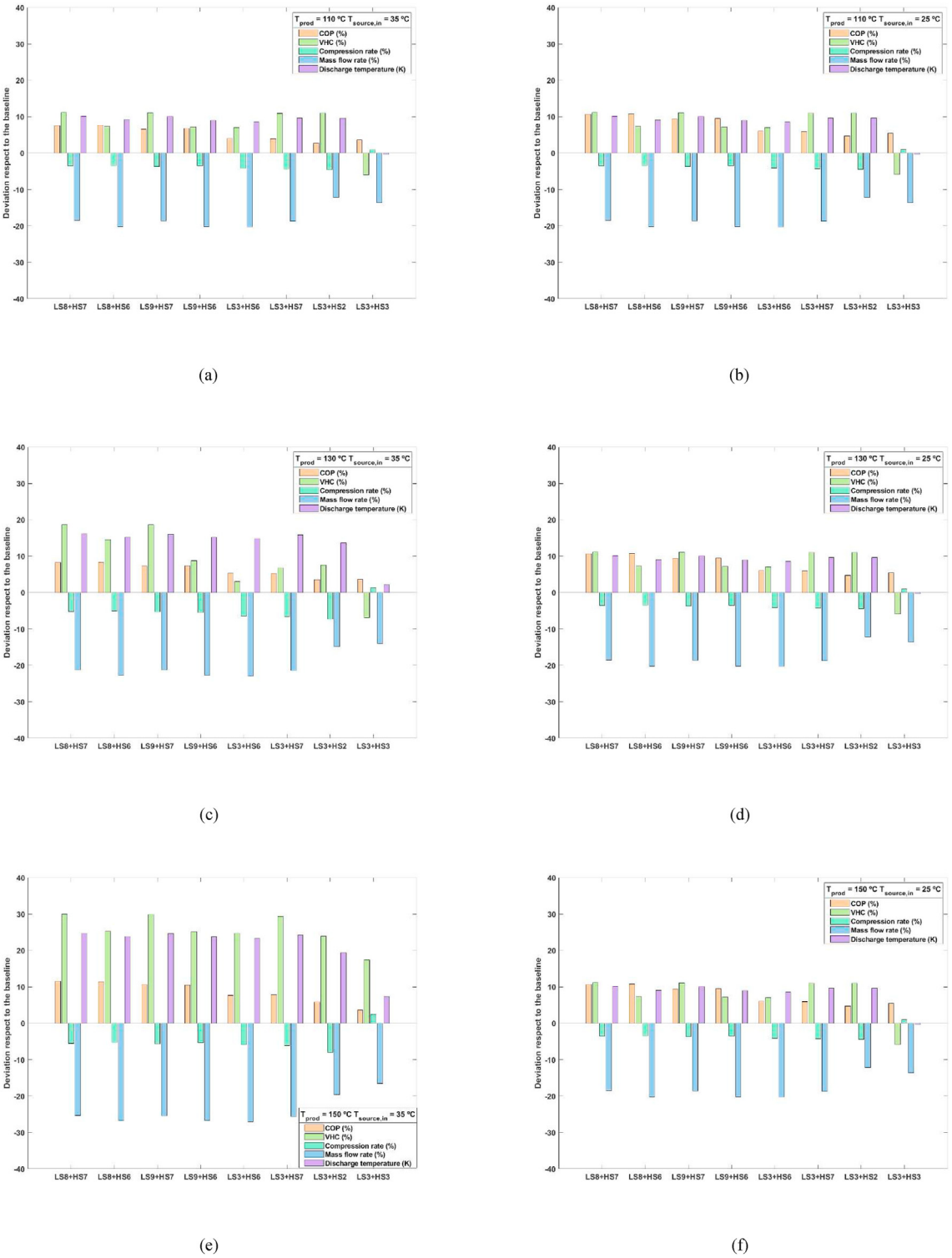

Fig. 9. Main parameters of the best combination of mixtures for six different boundary conditions.

goes from 5.0% for the baseline to 12.2% for the proposed combinations. Additionally, in a country with a small emissions factor, such as Sweden, the reduction in emissions is down to 72.0%.

It can be concluded that from an environmental point of view, the use of the combinations would suppose a remarkable reduction in carbon emissions for several countries. The use of low-GWP refrigerants is essential, but it is also crucial to use the mixture that best fits the temperature needs for an efficient and environmental-friendly system.

Table 8
Energy performance results of the baseline cascade.

Property	Value
Cycle	Baseline cascade
Refrigerants	R-1234ze(E) LS + R-1336mzz(Z) HS
COP	1.79
Heating capacity [kW]	10
Power consumption [kW]	5.59
Operating hours per year	8000
Annual consumption [kWh]	44692.7

Table 9
Carbon emission factor per country.

Country	Sweden	Finland	Spain	Italy	Netherlands	Poland
Carbon emission [$kgCO_2e\ kWh^{-1}$]	0.012	0.136	0.220	0.339	0.452	0.791

Table 10
Energetic and environmental results of the natural gas boiler.

Parameter	Value
Heating capacity [kW]	10
Operating hours per year	8000
Fuel consumption ratio [$kWh\ Nm^{-3}$]	10.65
Annual fuel consumption [Nm^{-3}]	7511.7
Fuel consumption ratio [$kgCO_2e\ Nm^{-3}$]	2.15
Annual carbon footprint [$kg\ CO_2e$]	16150.2

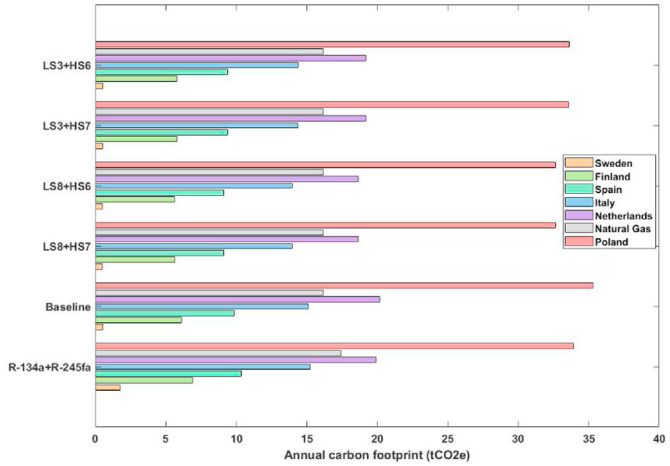

Fig. 10. Annual carbon footprint assessment considering the baseline and the different alternatives proposed.

Table 11
Emission reduction of the proposed combinations against R-134a + R-245fa emissions.

Working fluids	Sweden	Finland	Spain	Italy	Netherlands	Poland
Baseline	69.66%	11.61%	4.97%	0.76%	Increase	Increase
LS8+HS7	71.96%	18.30%	12.17%	8.27%	6.32%	3.71%
LS8+HS6	71.98%	18.36%	12.23%	8.33%	6.39%	3.78%
LS3+HS7	71.17%	16.02%	9.71%	5.70%	3.70%	1.02%
LS3+HS6	71.14%	15.91%	9.60%	5.58%	3.58%	0.90%

6. Conclusions

This paper assesses the potential of two-stage cascade heat pumps competing with natural gas boilers and promoting industry decarbonization. As there is still room for improvement for the alternative options that provide high thermal levels above 100 °C, different combinations of novel refrigerants in high- and low-temperature stages are tested and proposed on a semi-empirical approach for six different relevant temperature scenarios. The refrigerants were selected through a literature revision of potential mixtures for medium scale heat pump applications for the low stage and high temperature heat pump mixtures for the high stage.

A two-stage cascade model was developed using R-1234ze(E) and R-1336mzz(Z) data for LS and HS. For this, experimental measurements of both cycles were performed separately for covering reasonable temperature lifts from ambient to outlet sink temperature. The semi-empirical models for both cycles provided a deviation below 10%, and thus, the model was validated.

Then, novel refrigerant mixtures (still not registered in the ASHRAE standard 34) were taken from previous articles that identified them as promising in terms of energy performance. The energy performance of these refrigerants, classified according to the temperature level they aim for, was studied based on the semi-empirical model, adapting new equations. All proposed alternatives have a low GWP, but their flammability class is variable.

The combination with the highest COP was R-600/R-152a (0.08/0.92) with R-1233zd(E)/R-161 (0.88/0.12) for LS and HS, respectively. However, the LS fluid is highly flammable. Another combination that satisfies the flammability concern is R-1234ze(E)/R-32 (0.7/0.3), with lower COP than the first proposed combination but still higher than the baseline. HS mixtures showed a relevant increase in discharge temperature, so the IHX effectiveness should be limited to not exceeding 175 °C. The COP increase of the proposed mixtures is remarkable but not excellent. However, the increase in VHC is up to 30%. Future studies must consider different architectures for obtaining better results for efficiency.

As low GWP refrigerants are proposed, the only relevant HTHP contribution to global warming is the indirect emissions caused by the compressor power consumption. The HTHP cascade system is a competitive solution against natural gas boilers in countries with lower carbon emissions. Still, the conclusion is the opposite for Poland or The Netherlands.

To sum up, the energy performance of two-stage cascade HTHPs can be improved with novel mixtures still not registered. Moreover, LS fluids with high critical temperatures and lubricants that work at high temperatures are necessary since a higher intermediate cascade temperature benefits the overall COP. However, more efforts must be devoted to continuing with a green transition regarding the carbon emission factor of the electricity generation to increase the environmental and economic competitivity of HTHPs compared to natural gas boilers.

Declaration of competing interest

The authors declare that they have no known competing financial interests or personal relationships that could have appeared to influence the work reported in this paper.

Acknowledgements

The authors acknowledge the Spanish Government for the financial support under project RTC-2017-6511-3. Furthermore, the authors acknowledge the Universitat Jaume I (Castelló de la Plana, Spain) for the financial support under the projects UJI-B2018-24. Adrián Mota-Babiloni acknowledges grant IJC2019-038997-I funded by MCIN/AEI/10.13039/501100011033.

References

[1] Arpagaus C, Bless F, Uhlmann M, Schiffmann J, Bertsch SS. High temperature heat pumps: market overview, state of the art, research status, refrigerants, and application potentials, vol. 152; 2018.
[2] Kosmadakis G. Estimating the potential of industrial (high-temperature) heat pumps for exploiting waste heat in EU industries. Appl Therm Eng 2019;156:287–98. https://doi.org/10.1016/J.APPLTHERMALENG.2019.04.082.
[3] Kosmadakis G, Arpagaus C, Neofytou P, Bertsch S. Techno-economic analysis of high-temperature heat pumps with low-global warming potential refrigerants for upgrading waste heat up to 150 °C. Energy Convers Manag 2020;226:113488. https://doi.org/10.1016/j.enconman.2020.113488.
[4] Urbanucci L, Bruno JC, Testi D. Thermodynamic and economic analysis of the integration of high-temperature heat pumps in trigeneration systems. Appl Energy 2019;238:516–33. https://doi.org/10.1016/J.APENERGY.2019.01.115.
[5] Barco-Burgos J, Bruno JC, Eicker U, Saldaña-Robles AL, Alcántar-Camarena V. Review on the integration of high-temperature heat pumps in district heating and cooling networks. Energy 2022;239:122378. https://doi.org/10.1016/J.ENERGY.2021.122378.
[6] Sharan P, McTigue JD, Yoon TJ, Currier R, Findikoglu AT. Energy efficient supercritical water desalination using a high-temperature heat pump: a zero liquid discharge desalination. Desalination 2021;506:115020. https://doi.org/10.1016/J.DESAL.2021.115020.
[7] Cooper SJG, Hammond GP, Hewitt N, Norman JB, Tassou SA, Youssef W. Energy saving potential of high temperature heat pumps in the UK Food and Drink sector. Energy Proc 2019;161:142–9. https://doi.org/10.1016/J.EGYPRO.2019.02.073.
[8] Wu Z, Wang X, Sha L, Li X, Yang X, Ma X, et al. Performance analysis and multi-objective optimization of the high-temperature cascade heat pump system. Energy 2021;223:120097. https://doi.org/10.1016/J.ENERGY.2021.120097.
[9] Jung HW, Kang H, Yoon WJ, Kim Y. Performance comparison between a single-stage and a cascade multi-functional heat pump for both air heating and hot water supply. Int J Refrig 2013;36:1431–41. https://doi.org/10.1016/J.IJREFRIG.2013.03.003.
[10] Zou H, Li X, Tang M, Wu J, Tian C, Butrymowicz D, et al. Temperature stage matching and experimental investigation of high-temperature cascade heat pump with vapor injection. Energy 2020;212:118734. https://doi.org/10.1016/J.ENERGY.2020.118734.
[11] Xu L, Li E, Xu Y, Mao N, Shen X, Wang X. An experimental energy performance investigation and economic analysis on a cascade heat pump for high-temperature water in cold region. Renew Energy 2020;152:674–83. https://doi.org/10.1016/J.RENENE.2020.01.104.
[12] Bergamini R, Jensen JK, Elmegaard B. Thermodynamic competitiveness of high temperature vapor compression heat pumps for boiler substitution. Energy 2019;182:110–21. https://doi.org/10.1016/j.energy.2019.05.187.
[13] Wu D, Hu B, Wang RZ, Fan H, Wang R. The performance comparison of high temperature heat pump among R718 and other refrigerants. Renew Energy 2020;154:715–22. https://doi.org/10.1016/j.renene.2020.03.034.
[14] Mikielewicz D, Wajs J. Performance of the very high-temperature heat pump with low GWP working fluids. Energy 2019;182:460–70. https://doi.org/10.1016/J.ENERGY.2019.05.203.
[15] Frate GF, Ferrari L, Desideri U. Analysis of suitability ranges of high temperature heat pump working fluids. Appl Therm Eng 2019;150:628–40. https://doi.org/10.1016/J.APPLTHERMALENG.2019.01.034.
[16] Yan H, Ding L, Sheng B, Dong X, Zhao Y, Zhong Q, et al. Performance prediction of HFC, HC, HFO and HCFO working fluids for high temperature water source heat pumps. Appl Therm Eng 2021;185:116324. https://doi.org/10.1016/j.applthermaleng.2020.116324.
[17] Zhang X, Xu H. Experimental performance of moderately high temperature heat pump with working fluid R1234ze(Z). J Therm Anal Calorim 2021;144:1535–45. https://doi.org/10.1007/s10973-020-09610-1.
[18] Luo B, Zou P. Performance analysis of different single stage advanced vapor compression cycles and refrigerants for high temperature heat pumps. Int J Refrig 2019;104:246–58. https://doi.org/10.1016/J.IJREFRIG.2019.05.024.
[19] Malavika S, Chiranjeevi C, Raja Sekhar Y, Srinivas T, Natarajan M, Pa Pa Myo W, et al. Performance optimization of a heat pump for high temperature application. Mater Today Proc 2020. https://doi.org/10.1016/j.matpr.2020.08.639.
[20] Mateu-Royo C, Mota-Babiloni A, Navarro-Esbrí J. Semi-empirical and environmental assessment of the low GWP refrigerant HCFO-1224yd(Z) to replace HFC-245fa in high temperature heat pumps. Int J Refrig 2021;127:120–7. https://doi.org/10.1016/j.ijrefrig.2021.02.018.
[21] Jiang J, Hu B, Wang RZ, Liu H, Zhang Z, Li H. Theoretical performance assessment of low-GWP refrigerant R1233zd(E) applied in high temperature heat pump system. Int J Refrig 2021. https://doi.org/10.1016/j.ijrefrig.2021.03.026.
[22] Dai B, Liu X, Liu S, Zhang Y, Zhong D, Feng Y, et al. Dual-pressure condensation high temperature heat pump system for waste heat recovery: energetic and exergetic assessment. Energy Convers Manag 2020;218:112997. https://doi.org/10.1016/j.enconman.2020.112997.
[23] Mateu-Royo C, Arpagaus C, Mota-Babiloni A, Navarro-Esbrí J, Bertsch SS. Advanced high temperature heat pump configurations using low GWP refrigerants for industrial waste heat recovery: a comprehensive study. Energy Convers Manag 2021;229:113752. https://doi.org/10.1016/j.enconman.2020.113752.
[24] Mateu-Royo C, Mota-Babiloni A, Navarro-Esbrí J, Peris B, Molés F, Amat-Albuixech M. Multi-objective optimization of a novel reversible High-Temperature Heat Pump-Organic Rankine Cycle (HTHP-ORC) for industrial low-grade waste heat recovery. Energy Convers Manag 2019;197:111908. https://doi.org/10.1016/j.enconman.2019.111908.
[25] Xu C, Yang H, Yu X, Ma H, Chen M, Yang M. Performance analysis for binary mixtures based on R245fa using in high temperature heat pumps. Energy Convers Manag X 2021;12:100123. https://doi.org/10.1016/J.ECMX.2021.100123.
[26] Ma X, Zhang Y, Fang L, Yu X, Li X, Sheng Y, et al. Performance analysis of a cascade high temperature heat pump using R245fa and BY-3 as working fluid. Appl Therm Eng 2018;140:466–75. https://doi.org/10.1016/J.APPLTHERMALENG.2018.05.052.
[27] Zühlsdorf B, Jensen JK, Cignitti S, Madsen C, Elmegaard B. Analysis of temperature glide matching of heat pumps with zeotropic working fluid mixtures for different temperature glides. Energy 2018;153:650–60. https://doi.org/10.1016/J.ENERGY.2018.04.048.
[28] Mateu-Royo C, Mota-Babiloni A, Navarro-Esbrí J, Barragán-Cervera Á. Comparative analysis of HFO-1234ze(E) and R-515B as low GWP alternatives to HFC-134a in moderately high temperature heat pumps. Int J Refrig 2021;124:197–206. https://doi.org/10.1016/j.ijrefrig.2020.12.023.
[29] Thu K, Takezato K, Takata N, Miyazaki T, Higashi Y. Drop-in experiments and exergy assessment of HFC-32/HFO-1234yf/R744 mixture with GWP below 150 for domestic heat pumps. Int J Refrig 2021;121:289–301. https://doi.org/10.1016/J.IJREFRIG.2020.10.009.
[30] Yu B, Ouyang H, Shi J, Liu W, Chen Jiangping. Evaluation of low-GWP and mildly flammable mixtures as new alternatives for R410A in air-conditioning and heat pump system. Int J Refrig 2021;121:95–104. https://doi.org/10.1016/j.ijrefrig.2020.09.018.
[31] Li H, Tang K. A comprehensive study of drop-in alternative mixtures for R134a in a mobile air-conditioning system. Appl Therm Eng 2022;203:117914. https://doi.org/10.1016/J.APPLTHERMALENG.2021.117914.
[32] Calleja-Anta D, Nebot-Andrés L, Catalán-Gil J, Sánchez D, Cabello R, Llopis R. Thermodynamic screening of alternative refrigerants for R290 and R600a. Result Eng 2020;5. https://doi.org/10.1016/j.rineng.2019.100081.
[33] Fernández-Moreno A, Mota-Babiloni A, Giménez-Prades P, Navarro-Esbrí J. Optimal refrigerant mixture in single-stage high-temperature heat pumps based on a multiparameter evaluation. Sustain Energy Technol Assessments 2022;52:101989. https://doi.org/10.1016/j.seta.2022.101989.
[34] Linteris GT, Bell IH, McLinden MO. An empirical model for refrigerant flammability based on molecular structure and thermodynamics. Int J Refrig 2019;104:144–50. https://doi.org/10.1016/j.ijrefrig.2019.05.006.
[35] Lemmon EW, Bell IH, Huber MI, McLinden MO. NIST standard reference database 23: reference fluid thermodynamic and transport properties – REFPROP, version 10.0. NIST 2018.
[36] Fernández-Moreno A, Mota-Babiloni A, Giménez-Prades P, Navarro-Esbrí J. Optimal refrigerant mixture in single-stage high-temperature heat pumps based on a multiparameter evaluation. Sustainable Energy Technologies and Assessments n.d.
[37] Klein S. Engineering equation solver. EES); 2006.
[38] Mateu-Royo C, Navarro-Esbrí J, Mota-Babiloni A, Molés F, Amat-Albuixech M. Experimental exergy and energy analysis of a novel high-temperature heat pump with scroll compressor for waste heat recovery. Appl Energy 2019;253:113504. https://doi.org/10.1016/j.apenergy.2019.113504.
[39] Mota-Babiloni A, Mateu-Royo C, Navarro-Esbrí J, Barragán-Cervera Á. Experimental comparison of HFO-1234ze(E) and R-515B to replace HFC-134a in heat pump water heaters and moderately high temperature heat pumps. Appl Therm Eng 2021;196:117256. https://doi.org/10.1016/j.applthermaleng.2021.117256.
[40] EKh Shungarov, Garanov SA. Comparison of the characteristics of low-temperature scroll compressors for heat pump applications. Chem Petrol Eng 2020;56:378–84. https://doi.org/10.1007/s10556-020-00784-x.